

Copyright is owned by the Author of the thesis. Permission is given for a copy to be downloaded by an individual for the purpose of research and private study only. The thesis may not be reproduced elsewhere without the permission of the Author.

SOME ASPECTS OF SOIL PHYSICS  
APPLICABLE TO TRICKLE IRRIGATION

A thesis presented in partial fulfillment  
of the requirements for the Degree of  
Master of Science  
in Soil Science at  
Massey University

EWAN RODERICK HARPER  
1983

## ABSTRACT

Irrigation of crops is one of the more widely used techniques to increase yields. Trickle irrigation is one such method and is more suited to horticultural crops. In New Zealand, with horticulture assuming more importance, appropriate methods of design and operation of trickle irrigation systems are required. In this study a simple approximation to Wooding's solution for steady infiltration from a shallow ponded source, much like that found under trickle emitters is examined. This may aid in irrigation design and practice. The approximation also allowed for the development of a method to concurrently measure the saturated hydraulic conductivity and sorptivity from simple field infiltration measurements with a minimum of soil disturbance. Saturated hydraulic conductivities and sorptivities are of great use in soil water studies in general.

A commercial trickle irrigation system was also examined to determine the suitability of such irrigation systems to particular soils, and to examine the present irrigation scheduling. The approximation to Wooding's solution was found to perform well in the field in many respects, particularly in determining steady ponded zone sizes. Ponded zone sizes are important in that they control the volume of soil wetted by irrigation to a large degree. Much of this agreement is due to the use of parameters determined by the simple field method developed from this theory. Sorptivities and saturated hydraulic conductivities obtained by this method were found to be more realistic for trickle irrigation than those determined by other existing methods. Systematic errors in these other methods, mainly soil disturbance and the concomitant creation of continuous flow paths for water, as well as soil smearing, are thought to be the main cause of this difference.

Temporal and spatial variation in soil physical properties are however, found to hinder the use of soil physics theory in the field. Macropores (due to soil biological activity) were found to profoundly influence infiltration processes and soil-water distribution. These effects were particularly marked for the site with a commercial trickle irrigation system. Here the efficiency of the present system is thought to be low, and evidence indicates that irrigation was in excess of plant requirements. The utility of Wooding's solution, and the method to measure soil physical parameters developed from this, is further demonstrated in this orchard.

## ACKNOWLEDGEMENTS

I express my sincere thanks to my supervisors Dave Scotter and Brent Clothier for their encouragement, direction and friendship over the considerable period of time it has taken for this study. Also to my parents for their support and unstinting attitude with cheque books. Thanks to John Kirkman for his efforts on my behalf, and the staff of Plant Physiology Division, DSIR, for their help and use of facilities.

Thanks also to F.Z., Sir Henry and Marty for the inspiration necessary.

For the typing (above and beyond the call of normal duty, in a precarious state) I wish to thank Liz Wills.

## TABLE OF CONTENTS

	Page
Abstract.....	ii
Acknowledgements.....	iv
Table of Contents.....	v
List of Figures.....	viii
List of Tables.....	xvii
List of Symbols.....	xix

## CHAPTER 1

TRICKLE IRRIGATION: BACKGROUND AND THEORY.....	1
1.1 INTRODUCTION.....	2
1.2 IRRIGATION.....	2
1.2.1 GENERAL INTRODUCTION.....	2
1.2.2 HIGH FREQUENCY IRRIGATION: THEORETICAL CONSIDERATIONS.....	3
1.2.3 BENEFITS AND DISADVANTAGES OF HIGH FREQUENCY IRRIGATION.....	5
1.2.4 TRICKLE IRRIGATION.....	7
1.3 SOIL PHYSICS THEORY APPROPRIATE TO TRICKLE IRRIGATION.....	14
1.3.1 INTRODUCTION.....	14
1.3.2 NUMERICAL SOLUTIONS.....	15
1.3.3 QUASI-ANALYTICAL AND ANALYTICAL SOLUTIONS.....	15
1.4 DESIGN AND OPERATION OF TRICKLE IRRIGATION SYSTEMS.....	28
1.5 CONCLUSIONS.....	28

## CHAPTER 2

MEASUREMENT OF THE SATURATED HYDRAULIC CONDUCT- IVITY, SATIATED MATRIC FLUX POTENTIAL AND SORPTIVITY.....	30
2.1 INTRODUCTION.....	31
2.2 EXISTING METHODS OF $K_s$ , $\phi_s$ AND SORPTIVITY MEASUREMENT.....	32
2.3 MATERIALS AND METHODS.....	34

2.3.1	INTRODUCTION.....	34
2.3.2	SITES.....	34
2.3.3	MEASURING $K_s$ USING EXISTING METHODS.....	34
2.3.4	TWIN RING METHOD OF MEASURING $K_s$ , $\phi_s$ AND SORPTIVITY.....	36
2.4	RESULTS AND DISCUSSION.....	39
2.4.1	WELL, CORE AND INFILTRMETER $K_s$ MEASUREMENTS.....	39
2.4.2	UNBUFFERED INFILTRATION RATES.....	44
2.4.3	CALCULATION OF $K_s$ , $\phi_s$ AND SORP- TIVITY USING THE TWIN RING METHOD...	46
2.4.4	DISCUSSION.....	54
2.5	CONCLUSIONS.....	57

### CHAPTER 3

THREE-DIMENSIONAL INFILTRATION FROM POINT SOURCES.....		59
3.1	INTRODUCTION.....	60
3.2	MATERIALS AND METHODS.....	60
3.2.1	EXPERIMENTAL TECHNIQUE.....	60
3.2.2	WATER CONTENT DISTRIBUTIONS.....	61
3.2.3	PONDED AND WET FRONT RADII.....	61
3.2.4	PREDICTED WET FRONT DEPTH.....	62
3.3	RESULTS.....	63
3.3.1	PONDED AND WETTED RADII.....	63
3.3.2	WATER CONTENT DISTRIBUTIONS.....	73
3.4	CONCLUSIONS.....	80

### CHAPTER 4

TRICKLE IRRIGATION OF THE MASSEY ORCHARD.....		81
4.1	INTRODUCTION.....	82
4.2	MATERIALS AND METHODS.....	83
4.2.1	MASSEY ORCHARD.....	83
4.2.2	TENSIOMETRY.....	84
4.2.3	WATER BALANCE FOR THE MASSEY ORCHARD	87
4.3	RESULTS AND DISCUSSION.....	92

4.3.1	TRICKLE IRRIGATION SYSTEM.....	92
4.3.2	WATER BALANCE RESULTS.....	93
4.3.3	ROOT-ZONE SOIL-WATER POTENTIAL DIST- RIBUTIONS.....	98
4.3.4	PRACTICAL USE OF INFILTRATION THEORY	105
4.4	CONCLUSIONS.....	109

## CHAPTER 5

CONCLUSIONS.....	113
------------------	-----

## APPENDIX I

SOIL PROFILE DESCRIPTIONS.....	116
--------------------------------	-----

## APPENDIX II

STATISTICAL METHODS AND SUMMARY OF EXPERIMENTAL RESULTS.....	119
A2.1 STATISTICAL METHODS.....	120
A2.2 SUMMARY OF EXPERIMENTAL RESULTS.....	121

## APPENDIX III

BASIC PHYSICAL PROPERTIES.....	126
A3.1 INTRODUCTION.....	127
A3.2 METHODS.....	127
A3.3 RESULTS.....	128
BIBLIOGRAPHY.....	130

## LIST OF FIGURES

	Page
Fig. 1.1 Poned radius ( $r_p$ ) as a function of infiltration time for two soils and two discharges. Results are from numerical simulation. After Bresler (1978).....	9
Fig. 1.2 Wetting front position as a function of infiltration water (in litres) indicated by the numbers labelling the lines, for two soils and two discharges. Results are from numerical simulation. After Bresler (1978).....	11
Fig. 1.3 Dimensionless matric flux potential ( $\Phi/\Phi_s$ ) for two values of $a$ plotted with dimensionless radius ( $R$ ) and depth ( $Z$ ). Increasing $a$ indicates a more rapidly decreasing hydraulic conductivity (i.e. coarser soil texture). Poned zones are shown by the dark areas from $R = 0$ to $R = 1$ . After Wooding (1968)...	22
Fig. 1.4 Total dimensionless flux ( $F$ ) versus $a$ . Calculated line is shown along with the approximation $F = 2\pi a + 4$ . Divergence of the solution series with various numbers of terms retained in calculations is also shown. After Wooding (1968).....	24

- Fig. 2.1 Unbuffered infiltration fluxes from 0.102m radius rings ( $q$ ) versus core  $k_s$  values for the same location. Data points below the line  $q = k_s$  are theoretically impossible.
- (a) Manawatu sandy loam  
 (b) Manawatu fine sandy loam I  
 (c) Manawatu fine sandy loam II  
 (d) Tokomaru silt loam..... 42
- Fig. 2.2 Field core permeameters from the Tokomaru silt loam site. Rhodamine dye stained areas indicate preferential flow down channels. These channels may be of limited continuity in situ, when preferential flow may not occur to the same extent..... 43
- Fig. 2.3 Observed changes in  $q$  with time for two 0.18m radius rings at the Manawatu sandy loam site (O and ●). Also shown are calculated curves from equations (2.10) and (2.11), and values of  $t_*$  and  $q$ . Average values of  $k_s$  and sorptivity from the twin ring analysis were used. The expected variation in  $q$  with  $\theta_n$  is also illustrated by the second curve from equation (2.10) with  $\theta_n = 0.22$ ..... 53
- Fig. 2.4 Observed changes in  $q$  with time for two 0.037m radius rings at the Manawatu fine sandy loam II site (O and ●). Also shown are calculated curves from equations (2.10) and (2.11), and values of  $t_*$  and  $q$ . Average values of  $k_s$  and sorptivity from the twin ring analysis were used. The expected variation in  $q$  with  $\theta_n$  is also illustrated by the

- Fig. 2.4 second curve from equation (2.11) with  
(cont)  $\theta_n = 0.30$ ..... 55
- Fig. 3.1 Trickle experiment on the Manawatu sandy loam, with  $Q = 2.6 \times 10^{-7} \text{ m}^3 \text{ s}^{-1}$ .  
(a) Plan outline of ponded zone with time.  
—Ponded zone. Numbers on lines identify time in minutes.  
---Wetted zone at completion of experiment ( $t = 90 \text{ min.}$ ).  
(b) Ponded (O) and wetted (x) radii with time, estimated from graphical integration off photographs..... 63
- Fig. 3.2 Trickle experiment on the Manawatu fine sandy loam I, with  $Q = 6.8 \times 10^{-7} \text{ m}^3 \text{ s}^{-1}$ .  
(a) Plan outline of ponded zone with time.  
—Ponded zone. Numbers on lines identify time in minutes.  
---Wetted zone at completion of experiment ( $t = 180 \text{ min.}$ ).  
(b) Ponded (O) and wetted (x) radii with time, estimated from graphical integration off photographs..... 64
- Fig. 3.3 Trickle experiment on the Manawatu fine sandy loam II. Two flow rates were used. First  $Q = 1.5 \times 10^{-7} \text{ m}^3 \text{ s}^{-1}$ , followed by  $Q = 4.6 \times 10^{-7} \text{ m}^3 \text{ s}^{-1}$ .  
(a) Plan outline of ponded zone for  $Q = 1.5 \times 10^{-7} \text{ m}^3 \text{ s}^{-1}$ .  
—Ponded zone. Numbers on lines identify time in minutes.  
---Wetted zone at completion of experiment ( $t = 90 \text{ min.}$ ).

- Fig. 3.3 (b) Poned (O) and wet front (x) radii with time. Figures identify whether radii are for first (1) or second (2) flow rate..... 65
- Fig. 3.4 Trickle experiment on the Manawatu fine sandy loam I, with  $Q = 7.2 \times 10^{-7} \text{ m}^3 \text{ s}^{-1}$ .  
 (a) 65 minutes after the beginning of irrigation. The poned radius is approximately 0.13m. Scale is in centimetres.  
 (b) 1100 minutes after the beginning of irrigation. The poned radius is now approximately 0.02m. Many worm castes are apparent. Scale is in centimetres..... 67
- Fig. 3.5 Trickle experiments (■) in relation to predicted poned radii from Wooding's equation (equation 1.14) for the Manawatu sandy loam. Average values of  $k_s$  and  $\phi_s$  from the twin ring analysis are used. Shaded area indicates the 95% confidence interval..... 70
- Fig. 3.6 Trickle experiments (■) in relation to predicted poned radii from Wooding's equation (equation 1.14) for the Manawatu fine sandy loam I. Average values of  $k_s$  and  $\phi_s$  from the twin ring analysis are used. Shaded area indicates the 95% confidence interval..... 71
- Fig. 3.7 Trickle experiments (■) in relation to predicted poned radii from Wooding's equation (equation 1.14) for the Manawatu fine sandy loam II. Average values of  $k_s$  and  $\phi_s$  from the twin ring

- Fig. 3.7 analysis are used. Shaded area indicates (cont). the 95% confidence interval..... 72
- Fig. 3.8 Water content distribution for a trickle experiment on the Manawatu sandy loam with  $Q = 7.2 \times 10^{-7} \text{ m}^3 \text{ s}^{-1}$ . Shown are measured  $(\theta - \theta_n)$  profiles under the emitter (O), 5cm from the emitter (x) and at the edge of the ponded zone 10cm from the emitter (●). The predicted wet front from equation (3.) is also shown. This experiment corresponds with that shown in Figure 3.1..... 75
- Fig. 3.9 Water content distribution for a trickle experiment on the Manawatu fine sandy loam I with  $Q = 6.8 \times 10^{-7} \text{ m}^3 \text{ s}^{-1}$ . Shown are measured  $(\theta - \theta_n)$  profiles under the emitter (O), 10cm from the emitter (x), and at the edge of the ponded wet front from equation (3.3) is also shown. This experiment corresponds with that shown in Figure 3.2..... 76
- Fig. 3.10 Water content distribution for a trickle experiment on the Manawatu fine sandy loam II. Two flow rates were used, first  $Q = 1.5 \times 10^{-7} \text{ m}^3 \text{ s}^{-1}$ , followed by  $Q = 4.6 \times 10^{-7} \text{ m}^3 \text{ s}^{-1}$ . Shown are measured  $(\theta - \theta_n)$  profiles under the emitter (O) and at the edge of the wetted zone 15cm from the emitter (●). The predicted wet front from equation (3.3) is also shown. This experiment corresponds with that shown in Figure 3.3..... 77
- Fig. 3.11 Trickle experiment on the Manawatu fine sandy loam II site. Rhodamine dye was used in the irrigation water to identify preferential flow paths..... 78

- Fig. 4.1 A multi-chambered pressure regulating emitter of the type used in the Massey Orchard. Note the numerous worm castes. 83
- Fig. 4.2 Location of tensiometers in the Massey Orchard, and method of calculation of for mercury menometer tensiometers.  
 (a) Cross-section along lateral showing tensiometer ( $\Psi$ ) and emitter ( $\blacktriangledown$ ) locations.  
 (b) Method of calculation of  $\Psi$  for mercury menometer tensiometers..... 85
- Fig. 4.3 Installed tensiometer cup. Note the close contact with the soil, and large apple tree roots. This tensiometer was located 0.5m from the tree at a depth of 0.25m..... 86
- Fig. 4.4 Schematic representation of the water balance (Section 4.2.3). Symbols, defined in the text, are as follows:  $E_p$  pan evaporation, RF rainfall, I irrigation ET evapotranspiration, f crop factor, St(n) soil-water storage on day n, TWHC total water holding capacity, d drainage, PWP permanent wilting point capacity.... 88
- Fig. 4.5 Emitter during irrigation. Note the spray from the emitter and the basin like ponded zone.
- Fig. 4.6 Calculated drainage (d), evapotranspiration (ET) and rainfall (histogram) for two periods from the water balance. Irrigation events are denoted by dark histogram along the top scale.  
 (a) Period from 10 to 17 January.  
 Irrigation every second day.

- Fig. 4.6 No drainage is predicted.  
(cont). (b) Period from 20 to 27 February.  
Daily irrigation..... 99
- Fig. 4.7 Tensiometer response at 0.25m depth for two periods. Tensiometers are located 0.25m from the emitter (—) toward the tree, and 0.5m from the emitter (---) toward the tree. Irrigation events are denoted by ● .  
(a) Period from 10 to 17 January.  
Irrigation every second day.  
(b) Period from 20 to 27 February.  
Daily irrigation..... 100
- Fig. 4.8 Tensiometer response at 0.5m depth for two periods. Tensiometers are located 0.25m from the emitter (—) toward the tree, and 0.5m from the emitter (---) toward the tree. Irrigation events are denoted by ● .  
(a) Period from 10 to 17 January.  
Irrigation every second day.  
(b) Period from 20 to 27 February.  
Daily irrigation..... 101
- Fig 4.9 Tensiometer response at 0.8m depth for two periods. Tensiometers are located under the emitter (—) and under the tree (---). Irrigation events are denoted by ● .  
(a) Period from 10 to 17 January.  
Irrigation every second day.  
(b) Period from 20 to 27 January.  
Daily irrigation..... 102
- Fig. 4.10 Instantaneous drainage fluxes at 0.38m depth 0.25m from the emitter (●) and 0.5m from the emitter (□) at midday.

Fig. 4.10 Irrigation events are denoted by dark histogram on top scale. (cont).  
 (a) Period from 10 to 17 January. Irrigation every second day.  
 (b) Period from 20 to 27 February. Daily irrigation..... 104

Fig. 4.11 Pondered radii from trickle emitters in the Massey Orchard in relation to predicted radii from Wooding's equation, (equation 1.14) using average values of  $k_s$  and  $\phi_s$  from the twin ring analysis. Data points are for emitters which spray water (■) and only trickle (○) water. Shaded area is the 68% confidence interval..... 106

Fig. 4.12 Comparison of measured and predicted soil-water potential distributions from Wooding's (1968) solution. Solid lines are measured potentials on 24 February. Broken lines are predicted from equation (4.5) and Figure 6e of Wooding (1968) with  $a = 1$ . Figures on lines are soil-water potential values in kPa. Dark region below emitter indicates the ponded zone..... 108

Fig. A2.1 Core permeameter  $k_s$  data from the Manawatu sandy loam. Shown are measured values (●) and log-transformed data (□). Lines shown are for ideal normal (---) and log-normal (—) distributions using statistics from Table A2.1. Correlation coefficients indicate a log-normal distribution to provide the best fit to data..... 124

Fig. A2.2 Unbuffered infiltration rates from 0.102m radius rings on the Tokomaru silt loam. Shown are measured values ( $\square$ ) and log-transformed data ( $\bullet$ ). Lines shown are for ideal normal (—) and log-normal (---) distributions using statistics from Table A2.2. Correlation coefficients ( $r_{xy}$ ) indicate a normal distribution to provide the best fit to data.

## LIST OF TABLES

	Page	
Table 1.1	Chronological list of two- and three-dimensional solutions of the moisture flow equation (equation 1.2) using the linearizing assumption of $k = k_s \exp(\alpha\psi)$ .....	20
Table 2.1	Saturated hydraulic conductivity data from Well, Core and Buffered Infiltrometer methods.....	40
Table 2.2	Unbuffered infiltration data for four sites.....	45
Table 2.3	Saturated hydraulic conductivity data from Twin Ring Analysis.....	47
Table 2.4	Sorptivity and Satiated Matric Flux Potential data from Twin Ring Analysis..	49
Table 2.5	Saturated hydraulic conductivity and satiated matric flux potential from regression of all ring data.....	50
Table 3.1	Comparison of Twin Ring and Trickle Experiment methods of measuring $k_s$ and $\phi_s$ , and the Upper Limit to $k_s$ from Trickle Experiments.....	68
Table 3.2	Total Irrigation Input and Measured Water Content Increase.....	79
Table 4.1	Parameters used in the water balance..	96
Table 4.2	Monthly total of Water Balance Components for period November 1980 to March 1981.....	97

		Page
Table 4.3	Sample calculations for the Manawatu fine sandy loam II using Wooding's equation to estimate ponded zone size.	111
Table A2.1	Saturated hydraulic conductivities: Distribution statistics.....	122
Table A2.2	Unbuffered infiltration rates from rings (Q): Distribution statistics....	123
Table A3.1	Basic Physical Properties.....	130

## LIST OF SYMBOLS

		UNITS
a	dimensionless parameter (equation 1.13)	-
C	correction for mercury depression in capillary tube	kPa
$C_k$	dimensionless parameter (equation 2.5)	-
$C_\phi$	dimensionless parameter (equation 2.7)	-
CV	coefficient of variation	-
d	drainage rate	mm day <sup>-1</sup>
D	soil-water diffusivity	m <sup>2</sup> s <sup>-1</sup>
$D_*$	constant soil-water diffusivity	m <sup>2</sup> s <sup>-1</sup>
$E_p$	pan evaporation	mm day <sup>-1</sup>
ET	evapotranspiration	mm day <sup>-1</sup>
f	empirical constant	-
F	dimensionless flux (equation 1.13)	-
G	probability density function	-
h	mercury height in capillary tube	m
H	ponding height in auger hole	m
I	irrigation rate	mm day <sup>-1</sup>
J	drainage flux (equation 4.1)	mm day <sup>-1</sup>
k	hydraulic conductivity function	m s <sup>-1</sup>
$k_n$	hydraulic conductivity at the antecedent water content	m s <sup>-1</sup>
$k_s$	saturated hydraulic conductivity	m s <sup>-1</sup>
n	sample size	-
N	sample size required to be within a set interval of the mean	-
p	porosity	-
PWP	permanent wilting point	mm
q	soil-water flux density	m s <sup>-1</sup>
q	steady-state soil-water flux density	m s <sup>-1</sup>
Q	flow or discharge rate	m <sup>3</sup> s <sup>-1</sup>
$Q_B$	buffered flow rate	m <sup>3</sup> s <sup>-1</sup>
r	radial distance	m
$r_e$	radius at which two terms of equation (1.14) are equal	m
$r_{max}$	maximum ponded radius when flow is due solely to gravity	m
$r_o$	cavity radius	m
$r_p$	ponded radius	m

		xx
		UNITS
$r_u$	steady-state ponded radius	m
$r_w$	wetted radius	m
$r_{xy}$	correlation coefficient	-
R	dimensionless radius	-
RF	rainfall rate	mm day <sup>-1</sup>
s	standard deviation	-
$s_e$	standard error	-
$s_{ln}$	log-normal distribution standard deviation	-
$S(\theta_s, \theta_n)$	sorptivity	m s <sup>-1/2</sup>
St(n)	soil-water storage on day n	mm
$\Delta St$	change in soil water storage	mm day <sup>-1</sup>
t	time	s
$t_*$	calculated characteristic time toward steady-state	s
T	time to steady-state	s
TWHC	total water holding capacity of soil	mm
W	water content increment from irrigation	m <sup>3</sup>
x	horizontal distance	m
$\bar{x}$	mean value	-
y	horizontal distance (normal to x)	m
z	depth	m
$z_w$	wet front depth	m
Z	dimensionless depth	-
$\alpha$	slope of the exponential conductivity function (equation 1.7)	m <sup>-1</sup>
$\theta$	volumetric water content	-
$\theta_{FC}$	volumetric water content at field capacity	-
$\theta_n$	antecedent water content	-
$\theta_s$	satiated water content	-
$\Delta\theta$	change in profile water content	mm
$\rho_b$	dry bulk density	kg m <sup>-3</sup>
$\rho_s$	particle density	kg m <sup>-3</sup>
$\phi$	matric flux potential (equation 1.5)	m <sup>2</sup> s <sup>-1</sup>
$\phi_s$	satiated matric flux potential (equation 1.10)	m <sup>2</sup> s <sup>-1</sup>

## UNITS

$\Psi$  soil-water potential  
 $\Psi_t$  total soil-water potential

kPa

kPa

CHAPTER 1

TRICKLE IRRIGATION: BACKGROUND AND  
THEORY

## 1.1 INTRODUCTION

Irrigation, either to increase existing yields, or to allow development of previously barren areas has been practiced since at least 4000 B.C. (Jensen, 1980). Traditional methods, such as flood and furrow irrigation comprise most of the world's irrigated area, estimated in 1977 to be 223 million ha (FAO, 1977). These traditional methods supply water to plants in such a way that often 40 to 60% of applied water may drain from the root zone (Raats, 1974). In such cases soil storage capacity and plant drought tolerance are of prime importance (Rawlins, 1973). Technological developments over the last century have resulted in "high frequency irrigation" systems, which supply small amounts of water regularly to the root zone. Examples of such systems are trickle or trickle-drip systems, and mini-sprinkler systems. These systems may result in reduced drainage losses and reduce dependence on soil and plant characteristics.

In areas where intensive horticulture is practiced, such as in New Zealand, trickle irrigation is one of the more commonly used high frequency irrigation systems. The total global area estimated to be irrigated by this method in 1979 was 130,000 ha (Bresler, 1977). With the increasing importance of horticulture, techniques of design and operation, and methods of assessing the suitability of such systems are required. In the following sections of this chapter the principles and benefits of high frequency irrigation are discussed. Soil physics theory applicable to trickle irrigation is also introduced.

## 1.2 IRRIGATION

### 1.2.1 GENERAL INTRODUCTION

Surface irrigation imposes two fundamental constraints on irrigation management (Rawlins and Raats, 1975). Firstly flow over the soil surface is required to distribute water, and so a minimum depth of water is needed simply to achieve uniform coverage. The large spatial

variability in infiltration rates, even over a small area (e.g. Nielsen et al. 1973; Vieira et al. 1981), also results in large amounts of water being necessary to recharge the soil evenly over the total irrigated area. Those areas with the lowest infiltration rate then determine the total depth of water needed. Secondly fixed labour and material costs are associated with each application. Both these constraints make it economically advantageous to decrease the number of applications, by increasing the time between irrigations. This method of irrigation scheduling, commonly used for flood, furrow and hand portable sprinkler systems, is termed low frequency irrigation. Use of this method requires a substantial soil-water storage capacity and may often rely on the drought tolerance of the crop (Rawlins, 1973). The major process within the irrigation cycle is plant (root) extraction of water.

More recently developed irrigation systems (e.g. trickle, basin, solid-set and centre-pivot spray irrigation systems) have little or no additional cost associated with each application, and may result in a more uniform distribution of water to the root zone. These systems can be operated more frequently so as to match plant water usage. This method of irrigation scheduling, termed high frequency irrigation (HFI), lessens the dependence on crop drought tolerance and soil storage capacity. The irrigation process is "infiltration dominated", in contrast to the "extraction dominated" low frequency irrigation systems discussed previously. The consequences of this fundamental change in irrigation method, with emphasis on trickle irrigation, are covered in the following sections.

#### 1.2.2. HIGH FREQUENCY IRRIGATION: THEORETICAL CONSIDERATIONS

The physical basis of the advantages (and disadvantages) obtained using HFI are discussed below. Specific advantages and disadvantages of trickle irrigation are discussed in the following sections.

High frequency irrigation has been examined, using simple one-dimensional analyses by Rawlins (1973), Raats (1974) and Rawlins and Raats (1975). The basis of these studies is that high frequency pulses of water (of the order of one per day) are dampened within a few centimeters of the source (Gardner, 1964; Zur and Savaldi, 1977). Steady flow can reasonably then be assumed to exist. The simplest of these analyses is that of Rawlins (1973), which assumes steady downward flow in a homogeneous soil, due solely to gravity (i.e. matric potential gradients are neglected). Steady evaporative demands are represented by a root water extraction pattern that is considered to decrease exponentially with depth. Exponential decreases in root density are frequently found in the field (Scotter, 1976). As water is extracted by roots, the volumetric water content ( $\theta$ ) decreases. Thus the flux downwards, which is considered numerically equal to the hydraulic conductivity ( $k$ ), also decreases. If the flux at the surface is far in excess of transpiration, there will be extensive drainage beyond the root zone (at some arbitrary depth of the exponential function). However, if the surface flux is matched to the transpiration demands, drainage losses can be small. Although  $\theta$  in the root zone can be high,  $k$  often decreases rapidly with decreasing  $\theta$ , so consequently drainage can be kept to a minimum. This is shown clearly in Figure 3 of Rawlins (1973), and is also demonstrated by Raats (1974) and Rawlins and Raats (1975).

These latter two analyses, although still assuming both steady surface fluxes and transpirational demands, as well as an exponential root water extraction function, also account for matric potential gradients. Both these analyses examine the effect of salts in the irrigation water as well. Effects such as active exclusion of solutes by roots, and soil-solute interactions which may be important (Nye, 1979) are however not included. It is found that soil solution salt concentrations can be kept low, in the order of 2 to 3 times the concentration of the irrigation water, by adjusting surface fluxes to allow

drainage of the concentrated salt solution. While salinity control is of little importance in New Zealand, the implications of this theory to root-zone fertilizer concentration are of significance. This is discussed briefly in later sections.

### 1.2.3 BENEFITS AND DISADVANTAGES OF HIGH FREQUENCY IRRIGATION

#### (a) Benefits:

The following list of benefits can accrue from HFI.

(i) High soil-water potential: As the frequency of irrigation increases, the time average soil-water potential increases. (Note that dry soils have more negative potentials.) Thus HFI eliminates the large fluctuations in soil-water potential ( $\Psi$ ) of low frequency irrigation (Bresler and Yaron, 1972). While some early studies indicate transpiration does not appear to decrease until the "Permanent Wilting Point" is reached (e.g. Veihmeyer and Hendrickson, 1927), these should be treated with caution. Evidence indicates that lowering of  $\theta$ , even at the wet end of the range, may lead to a reduction of photosynthesis and eventually in growth (Gardner and Millar, 1973). It is now generally accepted that crop growth only proceeds unimpaired when  $\theta$  is reasonably high (Bresler, 1977). Plant yield, and possibly product quality are only maximal when  $\theta$  is continually high (Slatyer, 1969; Hsiao, 1973), unless a stress period is necessary for differentiation or fruit set (Salter and Goode, 1967). High time average soil water contents may also lead to improved yields through extreme temperature fluctuations being reduced (Freeburg et al. 1974).

(ii) Reduced water usage: HFI techniques when properly managed can reduce water usage. As application rates can be kept low, drainage beyond the root zone can be restricted. Although the wetted soil volume is often restricted for some HFI methods (e.g. trickle and small spray systems), reducing water usage, this may have little or no detrimental effect on plant yield. Transpiration and

growth rates decline little with large decreases in wetted root volumes, (e.g. Black and West, 1974; Frith and Nichols, 1974). Water savings can also be made by irrigating at rates less than the soils ability to absorb free water. By maintaining unsaturated flow runoff is minimized and flow down macropores and its deleterious consequences (e.g. Thomas and Phillips, 1979) are reduced.

(iii) Use of otherwise unsuitable soils: As application rates can be tailored to meet evapotranspirative demands with little drainage, soils with low water holding capacities (e.g. coarse textured soils) can be irrigated. Saline soils can also be irrigated if application rates are sufficient to flush salts from the root zone.

(iv) Improved nutrient status: Both the above mentioned analyses and more complex models (e.g. Bresler, 1975) demonstrate that solutes can be either flushed from, or retained within the root zone depending on application rate relative to the soils permeability. With low frequency irrigation leaching may be extensive due to excess drainage during and immediately following irrigation. With high water contents both root penetration and nutrient diffusion to roots are also enhanced. (Rawlins and Raats, 1975).

(b) Disadvantages:

While the disadvantages listed below can be minimized by good management of HFI systems, they deserve consideration.

(i) Poor soil aeration: If water contents are maintained too high oxygen diffusion within the soil may be reduced. Elimination of soil oxygen (i.e. anaerobic root zone conditions) has been found to cause stomatal closure, even at optimal soil water potentials (Sojka and Stolzy, 1980). This can result in fruit drop (Salter and Goode, 1967), impaired yields (e.g. Gur et al. 1979) or possibly plant death.

(ii) Reduced rooting volumes: While reduced root volumes can operate effectively, plant anchorage may suffer as a consequence. With smaller root volumes crop susceptibility to irrigation system breakdown is also increased, and nutrient availability is decreased. Where irrigation is supplementary to rainfall these disadvantages may be negligible, with roots extending throughout large portions of the soil in response to natural water content distributions.

(iii) Salt accumulations: Salts may accumulate at the edge of wetted volumes when solute concentrations in the soil or irrigation water (e.g. when fertilizer is added) are high. In these cases it may be necessary to flush these accumulations at some stage to prevent rain washing them into the root zone, leading to osmotic shock (Bresler, 1977). This will be of more importance when irrigated volumes are small such as for trickle and mini-sprinkler installations.

#### 1.2.4 TRICKLE IRRIGATION

##### (a) Physical Aspects

Although trickle irrigation was originally developed as a subsurface method in glasshouses in Germany (Howell *et al.* 1980), it appears to first been applied outdoors in Israel in the early 1960's (e.g. Celestre, 1964). Trickle irrigation involves the slow application of water from an emitter onto the soil surface. As the emitters are attached to supply pipes, this method is more suited to row crops (e.g. orchards and vineyards) than to densely planted crops.

Application of water from a single point onto the soil surface leads to wetted soil volumes being restricted both radially and vertically. Soil surface physical properties are critical in determining the area over which infiltration will take place, and hence the wetted soil volume. While highly permeable soils may have very small ponded zones, infiltration almost occurring from a point source (e.g. Roth, 1974), most soils have a ponded zone

ranging from 10 cm to 1 m in diameter. The shape of this pond is controlled by surface topography. Pondered zones typically increase in size as infiltration proceeds, until a final steady-state is achieved, in response to declining matric potential gradients. An upper limit to the pondered zone size can be found simply by assuming matric potential gradients to be non-existent. In this case fluxes will be due solely to gravity and hence a maximum radius ( $r_{\max}$ ) is given by:

$$r_{\max} = (Q/\pi k_s)^{\frac{1}{2}}. \quad (1.1)$$

Here  $Q$  is emitter discharge (in  $\text{m}^3\text{s}^{-1}$ ).

In coarser textured soils  $k_s$  is frequently large, and the final pondered zone size small (see Figure 1.1). Increasing  $Q$  will lead to a larger pondered zone, although longer times are then required to attain a final size (Brandt et al. 1971; Bresler et al. 1971; Levin et al. 1979). In some field cases (Earl and Jury 1977) times to attain a steady pondered zone size are large, in excess of a day. This contrasts with numerical simulations and other field studies. This difference is thought to be due to surface slaking and crusting. Numerical simulations for soils with different textures show coarser soils to obtain steady pondered zone sizes more rapidly than finer soils (see Figure 1.1).

As mentioned, the size of the pondered zone is important in that it controls the wetted volume to a large extent. Adjusting  $Q$ , or the length of application will allow lateral flow to be controlled to some extent. Typically wetted zones (and water content distributions) in vertical cross-section are semi-circular at short times, and elliptical at long times when gravity begins to dominate flow patterns at shorter times, the vertical extent of flow is greater than that for finer soils. This is a response to both decreased capillarity and decreased pondered zone sizes for similar discharge rates. Similarly for higher  $Q$

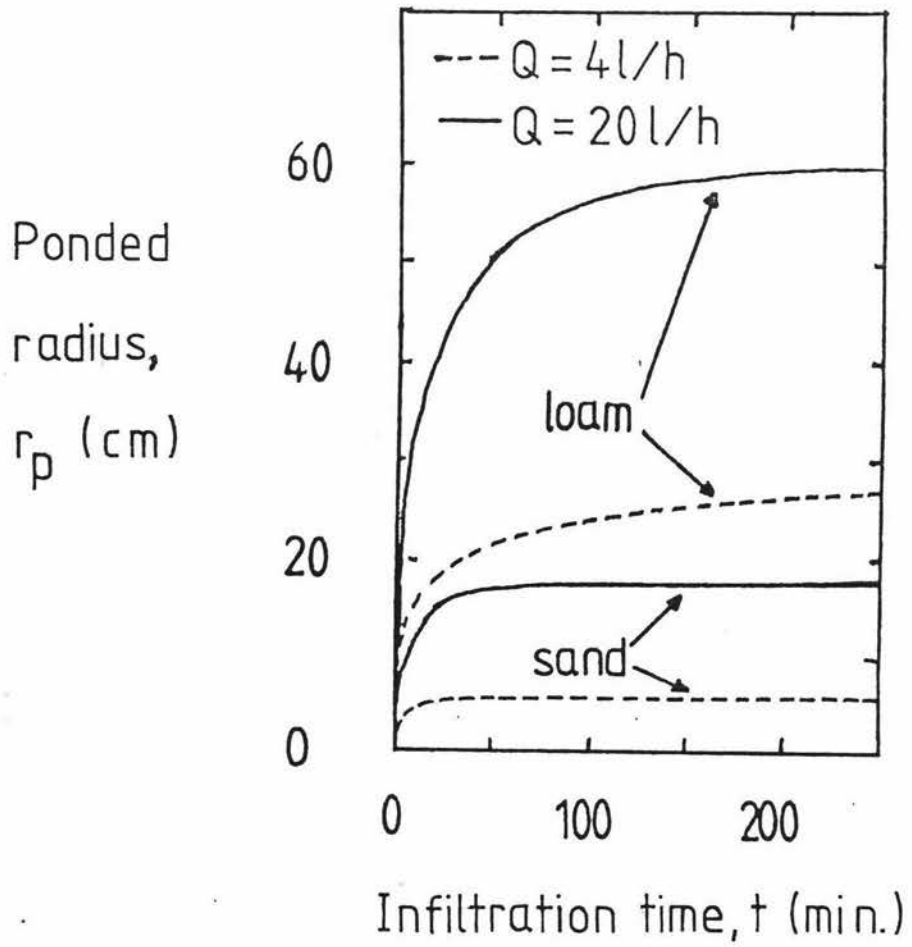


Fig. 1.1

Pondered radius ( $r_p$ ) as a function of infiltration time for two soils and two discharges. Results are from numerical simulation. After Bresler (1978).

wetted zones are shallower (for a given amount of water applied), due to increased ponded zone sizes. These trends are clearly seen in Figure 1.2. Total wetted soil volumes, however, decrease with decreasing  $Q$ , and the water content distribution within that volume tends to be more uniform (Levin et al. 1979).

Pulsing applications has a similar effect to lowering  $Q$  (Levin et al. 1979). In this case the steady ponded zone size is rapidly attained by sequential pulses due to a high antecedent water content ( $\theta_n$ ).

At the completion of irrigation, redistribution of the applied water begins. Little research has been carried out on redistribution from trickle sources, due to both the complexity of the process and the greater importance of infiltration. While vertical drainage is sometimes considered (e.g. Tsipori and Shimshi, 1979), the effect of lateral redistribution is generally neglected. While some studies indicate that lateral redistribution is generally neglected. While some studies indicate that lateral redistribution after irrigation is appreciable (e.g. Levin et al. 1979; Bar-Yosef and Sheikholslami, 1976; Mostaghimi et al. 1981), others demonstrate that this phenomenon may be of little consequence (e.g. Curtis and Watson, 1979). It appears likely that lateral redistribution will be of less significance in field situations, since wetted volumes are large, and large volumes of water are required to raise water contents by even small amounts at large distances away from the emitter.

Also in the field irrigation is usually frequent, whereas in many of the above studies irrigation was into an initially dry soil, so steady-state water content distributions may not have been attained. With frequent irrigation steady ponded zone sizes and wetted volumes are likely to be attained quickly.

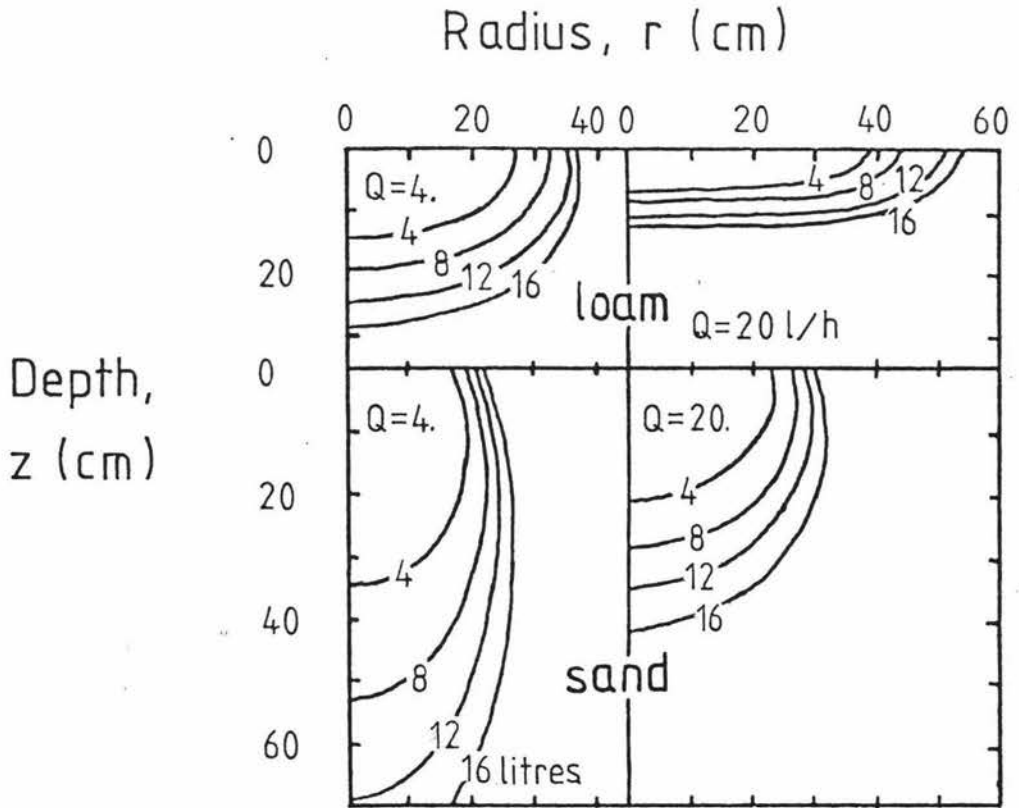


Fig. 1.2

Wetting front position as a function of infiltration time and cumulative infiltration water (in litres) indicated by the numbers labelling the lines, for two soils and two discharges. Results are from numerical simulation. After Bresler (1978).

While trickle irrigation shares the benefits (and drawbacks) of other HFI systems discussed previously, others are unique to this method. Some studies (e.g. Bresler, 1977; Howell et al. 1980; Bucks et al. 1982) have discussed these in detail. Salient points are listed below.

(b) Benefits

(i) Increased yields: While HFI often gives higher yields than low frequency irrigation, crop yields between high frequency irrigation methods, under similar management are comparable (e.g. Bernstien and Francois, 1973; Bucks et al. 1974; Hiler and Howell, 1973; Freeman et al. 1976). With adequate irrigation, increasing trickle irrigation frequency has been found to both increase (Goldberg and Shmueli, 1970; Levin et al. 1974) and to have no effect on yield (Earl and Jury, 1977). The above results highlight the need for efficient management of HFI systems. With efficient management trickle irrigation is one of the most useful methods of increasing crop yields (Tsipori and Shimshi, 1979), the flexibility in design available ( $Q$ , length of application, and emitter spacing and number all being variable) allows for a variety of configurations and crop factors to be accommodated.

(ii) Reduced water usage: Trickle irrigation restricts wetted zones horizontally. This can save water through reduced evapotranspiration and drainage from non-cropped areas. Run off and spray wind drift are non-existent (of sprinklers). Water may also be saved when crops are immature by lowering applications to wet smaller soil volumes (Howell et al. 1980).

(iii) Other factors: With trickle irrigation it is possible to fertilize or apply herbicides and fungicides directly to crop roots through the irrigation system. This can result in considerable savings of labour and materials (Bresler, 1977). Foliage is dry with trickle irrigation, and this may help to prevent leaf diseases that

rely on humidity for propagation. When emitters are located in rows, non-irrigated areas may be extensive. This allows freedom of movement for machinery. Labour costs can be reduced with automatic operation, and energy costs can be lower due to the low operational pressures required (Bresler, 1977).

(c) Drawbacks

(i) Emitter clogging: Emitters can be clogged if adequate filtering is not used. When there are few emitters per plant, this may have serious consequences for those plants which are adjacent to the affected emitter.

(ii) Cost: While trickle irrigation may be a low cost option for sparsely planted crops (Levin et al. 1974), the high cost of emitters can make it unsuitable for densely planted crops.

(iii) Small wetted areas: Considering the relatively small soil volume wetted by trickle irrigation, careful monitoring of soil water status is needed to maintain high yields, yet minimize drainage losses. For many crops, especially orchards, lysimeters are impractical due to the volume of soil in the root-zone of each plant (Howell et al. 1980). Techniques such as tensiometry, gravimetric sampling, neutron probing or the use of water balances are necessary. The problems associated with the use of these methods when wetted volumes are restricted are discussed in Chapter 4.

(iv) Design: To obtain the full benefits of trickle irrigation, system design is of paramount importance. The main design problem associated with trickle irrigation is selecting the proper combination of emitter spacing and discharge for a given soil and crop (Bresler, 1977; 1978). While several techniques already exist, it is best to use those based on physical theory, rather than solely on empirical methods, so design methods are more universally applicable. As infiltration is the dominant process in

trickle irrigation, theory describing the infiltration process is important. Existing theory which may be of use in designing and operating trickle irrigation systems is discussed in the following sections.

### 1.3 SOIL PHYSICS THEORY APPROPRIATE TO TRICKLE IRRIGATION.

#### 1.3.1 INTRODUCTION

Water distribution from a trickle source is best described using a three-dimensional geometry. For homogeneous, stable soil, combination of Darcy's law with a continuity expression gives the flow equation (Philip, 1969);

$$\partial\theta/\partial t = \nabla(k\nabla\Psi) - (\partial k/\partial z). \quad (1.2)$$

Here  $\theta$  is the volumetric water content,  $t$  is time,  $k$  is the unsaturated hydraulic conductivity,  $\Psi$  the matric potential, and  $z$  the vertical space co-ordinate, taken positive downward. The horizontal space co-ordinates are  $x$  and  $y$ . Radial co-ordinates, defining  $r = (x^2 + y^2)^{\frac{1}{2}}$ , can also be used if the flow is axis-symmetric.

Equation (1.2) can also be written in terms of the soil-water diffusivity,  $D$ , as;

$$\partial\theta/\partial t = \nabla(D\nabla\theta) - (dk/d\theta).(\partial\theta/\partial z). \quad (1.3)$$

The diffusivity is defined by;

$$D = k (d\Psi/d\theta). \quad (1.4)$$

Both  $D$  and  $k$  usually have a strong functional dependence on  $\theta$  (or  $\Psi$ ) and impart on equations (1.2) and (1.3) a highly non-linear nature. Unless simplifying assumptions are made, numerical techniques must be used to solve equations (1.2) and (1.3). Solutions which may be of use for trickle irrigation design and management are discussed in the following sections.

### 1.3.2 NUMERICAL SOLUTIONS

Equations (1.2) and (1.3) when applied to infiltration from a point source and subject to suitable initial conditions, can at present only be completely solved by numerical means. Three-dimensional infiltration was first simulated by Brandt et al. (1971), using both cylindrical and plane flow models, the source being a finite sized ponded zone expanding with time as matric-potential gradients decreased. While few comparisons have been made between numerical results and experimental data (Bresler, 1977), both field and laboratory studies show good agreement with this and similar models, (e.g. Bresler et al. 1971; Ben-Asher et al. 1978). Similar models have also been used (Bresler, 1975) to simulate simultaneous water and solute movement. Experimental evidence (Bresler and Russo, 1975; Levin et al. 1979) also validates this model. Redistribution can also be studied with these models, by simply extending calculations and accounting for hysteresis, so that the wetted portions begin to drain after cessation of irrigation (e.g. Curtis and Watson, 1979). Few, if any, simulations of three-dimensional infiltration with plant uptake have been undertaken. This is most probably due to the complexity of the processes involved. Results from numerical studies have been summarized and presented by Bresler (1977; 1978).

### 1.3.3 QUASI-ANALYTICAL AND ANALYTICAL SOLUTIONS

#### (a) Introduction:

Analytical solutions to the flow equation are those where the solution is found completely by mathematical analysis. Quasi-analytical solutions are those which have the basic form found by mathematical analysis, but some numerical means may have to be utilized to evaluate necessary coefficients or impressions (Philip, 1969). Most of the solutions outlined below are analytical (or exact) solutions.

Few, if any, analytical or quasi-analytical solutions for redistribution, root uptake or soil evaporation using three dimensional geometries are to be found in the literature. This may be due to the complexity of these phenomena. Existing one-dimensional solutions for plant uptake (e.g. Lomen and Warrick, 1978), drainage (Sisson et al. 1980), and evaporation (e.g. Gardner, 1958) may be used where emitter spacing and discharge is such that one dimensional flow effectively exists. Commonly used one-dimensional infiltration solutions (e.g. Philip, 1957) along with more recently developed theories such as that for pulsed flow (Zur and Savaldi, 1977) could also be used in such circumstances. However, where emitters are isolated, multi-dimensional infiltration solutions will be of more use. These are discussed below.

(b) Multi- dimensional transient absorption and infiltration solutions:

Much of the early infiltration theory is summarized by Philip (1969). The earliest multi-dimensional solution is that of Philip (1966) which models absorption (i.e. with gravity neglected) and infiltration from buried cavities. An exact series solution is given for absorption as well as two approximate solutions. The approximations concern the shape of the diffusivity function. Both "linear" (diffusivity constant with  $\theta$ ) and delta-function diffusivities (a Green and Ampt (1911) diffusivity) are used. These two diffusivities delineate the envelope of possible behaviour of all soils. Field and laboratory tests (Peck and Talsma, 1968; Talsma, 1969;1970) validate these solutions for short times. Transient and steady long time infiltration solutions using delta-function diffusivities are not given, being complex and of doubtful physical meaning (Philip, 1969). The exact solutions in a series form have not been used to date, as they require complex calculations and may only be useful for short times. Two- and three-dimensional long time steady infiltration solutions also exist (Philip, 1969) but have not been tested to date.